Free Radical Research, August 2010; 44(8): 913–924

Reactive oxygen species (ROS) reduce the expression of BRAK/CXCL14 in human head and neck squamous cell carcinoma cells

YOJIRO MAEHATA[1,2,*], SHIGEYUKI OZAWA[2,3,4,*], KYO KOBAYASHI[1,2], YASUMASA KATO[2,3], FUMIHIKO YOSHINO[1,2], CHIHIRO MIYAMOTO[1,2], KAZUHITO IZUKURI[2,3], EIRO KUBOTA[2,4], RYU-ICHIRO HATA[2,3] & MASAICHI-CHANG-IL LEE[1,2]

[1]*Department of Clinical Care Medicine Division of Pharmacology and ESR Laboratories,* [2]*Oral Health Science Research Center,* [3]*Department of Biochemistry and Molecular Biology, and* [4]*Department of Oral Maxillofacial Surgery, Kanagawa Dental College, Yokosuka, 238-8580, Japan*

(Received date: 28 December 2009; In revised form date: 26 April 2010)

Abstract

The present study investigated the effects of oxidative stress induced by reactive oxygen species (ROS), such as hydrogen peroxide (H_2O_2) and hydroxyl radical ($HO^•$), on the expression of both BRAK, which is also known as non-ELR motif angiostatic CXC chemokine ligand 14 (CXCL14), in head and neck squamous cell carcinoma (HNSCC) cells. When HNSCC cells were cultured in the presence of ROS, the expression of BRAK was significantly decreased whereas that of IL-8 was increased. Interestingly, the effects on the expression of both genes in HNSCC cells were much greater with $HO^•$ than with H_2O_2. The effects of ROS on both BRAK and IL-8 expression were attenuated by pre-treatment with N-acetyl-L-cysteine (NAC), epidermal growth factor receptor (EGFR), and mitogen-activated protein kinase (MAPK) inhibitors. These results indicate that oxidative stress induced by H_2O_2 or $HO^•$ stimulates angiogenesis and tumuor progression by altering the gene expression of BRAK and IL-8 via the EGFR/MEK/ERK pathway in human HNSCC cells.

Keywords: *Reactive oxygen species, BRAK, IL-8, H_2O_2, hydroxyl radical, HNSCC cell*

Abbreviations: *BRAK, breast and kidney-expressed chemokine; CXCL14, CXC chemokine ligand 14; DC, dendritic cells; DMEM, Dulbecco's modified Eagle's medium; DMPO, 5,5-dimethyl-1-pyrroline-N-oxide; DNTB, 5′-dithiobis-2-nitrobenzoic acid; EGFR, epidermal growth factor receptor; ESR, electron spin resonance; GAPDH, Glyceraldehyde 3-phosphate dehydrogenase; HNSCC, head and neck squamous cell carcinoma; H_2O_2, hydrogen peroxide; $HO^•$, hydroxyl radical; IL-8, Interleukin-8/CXCL8; MAPK, mitogen-activated protein kinase; MnO, manganese oxide; MTT, 3-(4,5-dimethyl-2-thiazolyl)-2,5-diphenyl-2H tetrazolium bromide; NAC, N-Acetyl-L-Cysteine; NADPH, nicotinamide adenine dinucleotide phosphate; NF-κB, nuclear factor kappa-B; ROS, reactive oxygen species; SCC, squamous cell carcinoma; $O_2^{•-}$, superoxide; TAMs, tumour-associated macrophages; TBS, Tris-buffered saline.*

Introduction

Reactive oxygen species (ROS) such as superoxide ($O_2^{•-}$), hydrogen peroxide (H_2O_2), and hydroxyl radical ($HO^•$), are formed *in vivo* and can act as powerful oxidizing agents, capable of damaging DNA and other biomolecules. Increased formation of ROS can promote the development of malignancy, and the physiological rates of ROS generation may account for the increased risk of cancer development associated with ageing [1]. It is possible that ROS act as critical angiogenic factors and participate closely in tumour initiation/progression. ROS stimulate production of the angiogenic chemokine IL-8 through activation of nuclear factor kappa-B (NF-κB) and

Correspondence: Masaichi-Chang-il-Lee, Department of Clinical Care Medicine Division of Pharmacology, Kanagawa Dental College, Yokosuka, 238-8580, Japan. Tel: +81-46-822-8836. Fax: +81-46-822-8868. Email: ieeman@kdcnet.ac.jp
*These authors contributed to this work.

ISSN 1071-5762 print/ISSN 1029-2470 online © 2010 Informa UK Ltd.
DOI: 10.3109/10715762.2010.490836

mitogen-activated protein kinase (MAPK) pathways in human head and neck squamous cell carcinoma (HNSCC) cells [2,3]. The direct influence of constitutive stimulation of ROS is not known but has been linked to angiogenic/angiostatic chemokines, particularly CXCL14/BRAK.

In contrast, non-ELR motif chemokines, such as angiostatic chemokine CXCL14/BRAK, have been reported to contribute to infiltration of B-cells, monocytes and dendritic cells (DC) into tumour tissues [4,5]. Generally, BRAK mRNA is abundantly expressed in normal tissues, but expression is absent or weak in certain carcinomas and carcinoma-cell lines, including HNSCC cells [6–8]. We previously demonstrated that BRAK has potent anti-tumour activity in HNSCC cells [8]. It is not yet known whether BRAK expression in tumour tissues is affected by the pericellular environment (e.g. hypoxia) and oxidative stress induced by ROS.

With respect to lung cancer, experimental studies in rats, as well as molecular epidemiological studies in humans, have provided evidence that the influx of inflammatory cells, such as neutrophils, into the airways may be an important process linking inflammation with carcinogenesis [9]. Tumours require a constant influx of other inflammatory cells such as tumour-associated macrophages (TAMs), which also play an important role in the *in vivo* induction of angiogenesis in HNSCC, to support the angiogenesis and stroma remodelling needed for tumour growth [10,11]. In addition to producing angiogenic chemokines, inflammatory cells also generate ROS such as $O_2^{\bullet -}$, H_2O_2 and $HO^{\bullet}$ via a plasma membrane-bound nicotinamide adenine dinucleotide phosphate (NADPH)-oxidase [12–14].

Since the discovery in 1991 that NF-κB may be activated by H_2O_2, several laboratories have put a substantial effort into analysing the molecular mechanisms underlying this activation [15]. Typically, studies on the effects of ROS in carcinoma cell lines have utilized H_2O_2. Challenging HSNCC cells with H_2O_2 has been shown to increase production of vascular endothelial growth factor and IL-8 [2]. TAMs may also generate $HO^{\bullet}$ from H_2O_2 via the Fenton/Haber-Weiss reaction catalysed by Fe^{2+} and Cu^{2+} in tumor tissue [16]. $HO^{\bullet}$ is a very potent oxidizing agent and its production has been shown to correlate with tumour development [1,14,17,18]; however it is not known whether H_2O_2 and $HO^{\bullet}$ have a direct effect on angiogenic chemokines such as IL-8 or BRAK involved in tumour-cell signalling.

It has been reported that epidermal growth factor receptor (EGFR) is highly expressed in a lot of types of carcinoma, including human HNSCC cells, and high level expression of EGFR decreases survival rates due to a strong prognostic indicator [19]. Moreover, ROS such as H_2O_2 stimulates production of angiogenic chemokine IL-8 through activation of NF-κB and MAPK including EGFR/MEK/ERK pathway in human HNSCC cells [2,3]. Recent studies suggest that $O_2^{\bullet -}$ and H_2O_2 are mitogenic mediators of activated growth-factor receptor signalling [20]. We previously reported that the expression of BRAK was down-regulated significantly in HNSCC cells treated with EGF [8]. Our laboratories previously developed an electron spin resonance (ESR)-based technique for the direct detection of ROS in biological systems [12,13,18,21–25]. In the present study, we found that ROS directly induced the angiogenesis of tumour progression to regulate the gene expression of angiostatic chemokine (BRAK)/angiogenic (IL-8) in HNSCC cells via the EGFR/MEK/ERK pathway in human HNSCC cells.

Materials and methods

Materials and reagents

Gefitinib (ZD 1839, Iressa) was kindly provided by AstraZeneca (Macclesfield, UK), Recombinant EGF and N-acetyl-L-cysteine (NAC) were purchased from Sigma (St. Louis, MO) and NAC stock was made in water and neutralized with 5 mol/L NaOH. Other reagents and their sources were the following: hydrogen peroxide (H_2O_2), $FeSO_4$, gentamicin sulphate, HEPES, trypsin, and EDTA from Wako Chemical (Osaka, Japan); 5,5-dimethyl-1-pyrroline-*N*-oxide (DMPO) from Labotec (Tokyo, Japan); Dulbecco's modified Eagle's medium (DMEM) from Nissui Seiyaku (Tokyo, Japan); Coulter Counter from Beckman Coulter (Fullerton, CA); foetal bovine serum from Trance Scientific (Melbourne, Australia); PD 98059, U-0126 and PD 153035 from Calbiochem (San Diego, CA); Fungizone, Super Script II reverse transcriptae, TRIzol total RNA isolation reagent, SuperScript First-strand Synthesis system and iBlot gel transfer stacks PVDF from Invitrogen (Carlsbad, CA); Ex Taq DNA polymerase from TaKaRa (Otsu, Japan); 2 × Full Velocity QPCR Master MiX from STRATAGENE (Tokyo, Japan); TaqMan Gene Expression Assay kits and MX3000P from STRATAGENE (Tokyo, Japan); Anti-phosphorylated ERK antibody, Anti-ERK antibody and RIPA buffer from Santa Cruz (CA, USA); Anti-phosphorylated EGFR antibody from Millipore (Mississauga, ON); Anti ERK antibody from Cell Signaling Technology (Beverly, MA); ECL™ Anti-rabbit horseradish peroxidase-linked whole antibody from Amersham (Buckinghamshire, UK); Lumi-Light Western Blotting substrate from Roche Molecular Biochemicals (Mannheim, Germany); CXCL14 Duo Set ELISA Development System kits from R&D Systems (Abington, UK); and Quanta Blue Fluorogenic Peroxidase Substrate Kit from Pierce (Rockford, IL).

In vitro *ESR measurement*

$HO^{\bullet}$ was generated by Fenton reaction (H_2O_2 + $FeSO_4$) as described previously [17,18,25]. All solutions were prepared in serum-free DMEM (DMEM-0). ESR spin-trapping was conducted with an ROS-generating system containing DMPO. ESR observations were performed with a JES-RE1X X-band spectrometer (JEOL, Tokyo, Japan) connected to a WIN-RAD ESR Data Analyser (Radical Research, Tokyo, Japan) at the following instrument settings: microwave power, 8.00 mW; magnetic field, 335.3 ± 5 mT or 334.7 ± 5 mT; field modulation width, 0.079 mT; receiver gain, 100–500; sweep time, 1 min; and time constant, 0.03 s. To quantify the spin adducts detected, we obtained ESR spectra for manganese oxide (MnO) standards. After the ESR spectra were recorded, the signal intensity, expressed as relative height, was normalized against the signal intensity of the MnO standard. All experiments were repeated a minimum of three times.

Cells and cell culture

The HNSCC cell lines used in this study were as follows: HSC-2 (oral floor), HSC-3 (tongue) and HSC-4 (tongue) [26]. These cell lines were provided by the Japanese Cancer Research Resources Bank (JCRB). The cells were cultured with DMEM in the presence of 50 μg/ml gentamicin sulphate, 250 ng/ml fangizone, 12.6 mM HEPES and 10% FBS at 37°C under 5% CO_2, and were sub-cultured by treatment with 0.25% trypsin. Cells were used within three or four passages. Cell numbers were counted with a Coulter Counter.

Measurement of total glutathione (GSH and GSSH)

Total glutathione (GSH and GSSH) levels in HSC-2 cells were quantified using the Total Glutathione Quantification Kit. HSC-2 cells were seeded (4×10^5 cells/well) on a 35-mm diameter dish. Nearly confluent cells were serum starved overnight. After incubation with or without NAC for 4 h, the cells were homogenized in 10 mM HCl and placed into a 96-well plate. Intracellular GSH and GSSH were reacted with 5'-dithiobis-2-nitrobenzoic acid (DNTB) and the absorbance was measured spectrophotometrically at 405 nm.

Cell viability axssay

HSC-2, HSC-3 and HSC-4 cells were seeded (5×10^3 cells/well) in 96-well plates. Nearly confluent cells were serum-starved overnight and cultured in DMEM-0 with various concentrations of H_2O_2, with or without $FeSO_4$, for 6 h. For the 3-(4,5-dimethyl-2-thiazolyl)-2,5-diphenyl-2H tetrazolium bromide (MTT) assay, we used Tetracolor One, a water-soluble derivative of MTT which is reduced to a formazan product by active mitochondrial enzymes in living cells. After adding 10 μl of the dye solution to each well, the plates were incubated for 120 min at 37°C. After incubation, a microplate reader was used to measure the absorbance at 450 nm. Absorbance values were expressed as a percentage of the absorbance for untreated cells, and the concentration of H_2O_2 with or without $FeSO_4$ resulting in 50% growth inhibition (IC_{50}) was calculated. All experiments were done in triplicate.

Reverse transcription-polymerase chain reaction (RT-PCR)

HNSCC cells were inoculated (4×10^5 cells/well) on a 35-mm diameter dish. After serum starvation overnight, the cells were cultured in DMEM-0 in the presence of H_2O_2 (250 μM) with or without $FeSO_4$ (250 μM) for 6 h. Total RNA (1 μg) was extracted using TRIzol total RNA isolation reagent and analysed for BRAK and IL-8 mRNA expression by RT-PCR. An aliquot of each sample was denatured and reverse transcribed by using a SuperScript First-strand Synthesis system according to the manufacturer's protocols. The PCR amplification was carried out on the RT reaction product with primers and 0.5 units of EX Taq polymerase. The primer sets used were as follows: BRAK (232 bp), -AATGAAGCCA AAGTACCCGC-3′-(forward) and 5′-AGTCCTTT GCACAAGTCTCC-3′ (reverse); IL-8 (342 bp), GCCAAGGAGTGCTAAAGAAC-(forward) and 5′-CATCTGGCAACCCTACAACA-3′ (reverse). Glyceraldehyde 3-phosphate dehydrogenase (GAPDH) mRNA was co-amplified as an internal control [752 bp, 5′-GTGAAGGTCGGAGTCAACGG-3′ (forward) and 5′-GGCAGGTTTTTCTAGACGGC-3′ (reverse)]. The PCR products were separated on 2% agarose gel and visualized by ethidium bromide staining as previously reported [27].

Real-time RT-PCR analysis

Complementary DNAs were prepared by using a SuperScript First-strand Synthesis system and real-time PCR was performed with 2 × FullVelocity QPCR Master MiX and TaqMan Gene Expression Assay kits. Amplifications were carried out using an MX3000P PCR apparatus for 40 cycles after initial denaturation at 95°C for 2 min. The standard reaction conditions were 95°C for 10 s for denaturation and 60°C for 30 s for annealing and polymerization. The following specific primers were used: Hs99999905_m1 for GAPDH; Hs00171135_m1 for CXCL14/BRAK; and Hs00174103_m1 for CXCL8/IL-8. For analysis of PCR products by gel

electrophoresis, the PCR conditions were 94°C for 2 min followed by 17–24 cycles at 95°C for 10 s, annealing at 60°C for 30 s and polymerization at 72°C for 30 s. PCR products were visualized by staining with ethidium bromide after separation by agarose gel electrophoresis.

Protein quantification

HNSCC cells were inoculated (4×10^5 cells/well) on a 35-mm diameter dish. After being serum-starved overnight, these cells were cultured in DMEM-0 with the presence of H_2O_2 (250 μM) with or without $FeSO_4$ (250 μM) for 48 h. These cells were isolated with RIPA buffer. Culture medium was also collected and concentrated with cold acetone, samples were diluted in RIPA buffer. These protein levels of BRAK were quantified using CXCL14 Duo Set ELISA Development System kits following the manufacturer's instruction, except for the detection step that used a Quanta Blue Fluorogenic Peroxidase Substrate Kit.

Western blotting

HNSCC cells were inoculated (4×10^5 cells/well) on a 35-mm diameter dish. After serum starvation overnight, the cells were cultured in DMEM-0 in the presence of H_2O_2 (250 μM) with or without $FeSO_4$ (250 μM) for various incubation times (0.25, 0.5, 1, 2, 4 h). Samples were boiled for 10 min at 100°C prior to electrophoresis on 4–20% gradient polyacrylamide gels. Proteins were transferred onto a PVDF membrane using the iBlot dry blotting system at constant voltage of 20 volts for 8 min. The blots were blocked in 3% non-fat dry milk in Tris-buffered saline (TBS) with 0.05% Tween20 for 1 h at room temperature, and then incubated with primary antibodies overnight at 4°C in blocking solution. The dilution factors for the primary antibodies were as follows: p-EGFR (polyclonal, 1:200), EGFR (polyclonal, 1:200), p-ERK1/2 (polyclonal, 1:100), ERK (polyclonal, 1:100). Secondary antibodies, goat ECL™ anti-rabbit horseradish peroxidase-linked whole antibody were diluted 1:2000 in blocking solution (3% non-fat dry milk in TBS containing 0.05% Tween 20). The blots were washed and incubated with secondary antibodies for 1 h at room temperature in blocking solution. Immunoreactive bands were visualized by using Lumi-Light western blotting substrate.

Statistical analysis

Results are expressed as mean ± SD. Statistical analysis was performed using Student's *t*-test or one-way analysis of variance. A *p*-value less than 0.05 was considered to be statistically significant.

Results

Determination of hydroxyl radical (HO•) in culture medium using X-band ESR measurement

In the current study, HO• was generated using the Fenton reaction and detected using the X-band ESR spin trapping technique with DMPO as the spin trap [17,18,25]. We observed the characteristic ESR spectra of DMPO-OH spin adduct with hyperfine splitting giving rise to four resolved peaks (Figure 1A), indicative of HO• generation. The top spectrum is a computer-simulated spectrum for the DMPO-OH spin adduct. The spectra obtained from Fenton reaction with different concentrations of H_2O_2 or $FeSO_4$ (0–250 μM) were observed. Figure 1B shows the signal intensity of the second peak of the spectrum which was normalized to the peak height of the MnO standard. The signal intensity was increased in a dose-dependent manner in the presence of H_2O_2 or $FeSO_4$. To investigate the time dependency of HO• generation, we used 250 μM H_2O_2 or $FeSO_4$ (Figures 1C and D). As shown in Figure 1C, DMPO-OH spin adducts were observed at 1, 2, 4, 5 and 30 min after addition of H_2O_2. The relative amount of HO• decreased in a time-dependent manner (Figure 1D).

Furthermore, we examined the IC_{50} of HNSCC cells to ascertain whether the concentrations of ROS in our studies had an inhibitory effect on cell proliferation. The IC_{50} of HNSCC cells was determined by MTT assay after treatment with H_2O_2 and HO• (H_2O_2/$FeSO_4$) for 24 h. The average IC_{50} against H_2O_2 was: HSC-2 (849 ± 71 μM), HSC-3 (495 ± 19 μM) and HSC-4 (648 ± 11 μM) and the average IC_{50} against HO• (H_2O_2/$FeSO_4$) was: HSC-2 (849 ± 71 μM), HSC-3 (495 ± 19 μM) and HSC-4 (648 ± 11 μM). These concentrations (0–250 μM) of H_2O_2 and/or $FeSO_4$ which were used for ROS treatment in our studies were much lower than the growth-inhibitory dose (Figure 1E).

Reactive oxygen species (ROS) decrease the expression of the angiostatic chemokine BRAK in human HNSCC cells

It has been previously reported that ROS (i.e. H_2O_2) increase the expression of the angiogenic chemokine IL-8 via activation of MAPK and NF-κB pathways in HNSCC cells [2]. In order to investigate ROS-mediated rupture mechanisms via regulation of BRAK expression, we examined the expression of BRAK using real-time PCR analysis in HNSCC cells treated with H_2O_2 and HO•. We confirmed that IL-8 mRNA levels were significantly increased by treatment with H_2O_2 in three kinds of HNSCC cells. On the other hand, BRAK mRNA levels were significantly decreased by H_2O_2 treatment. Interestingly, the effects of HO• treatment on the expression of both angiogenesis related-chemokine genes were much

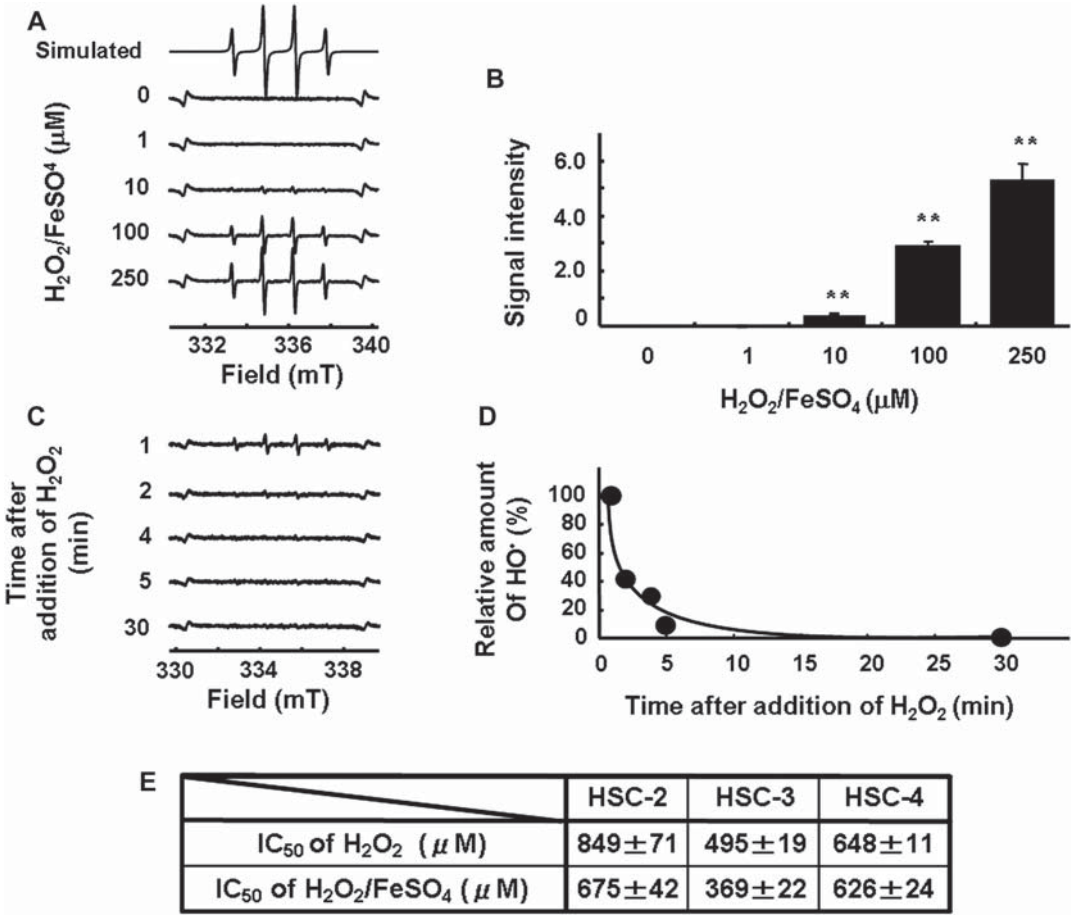

E

	HSC-2	HSC-3	HSC-4
IC_{50} of H_2O_2 (μM)	849±71	495±19	648±11
IC_{50} of H_2O_2/$FeSO_4$ (μM)	675±42	369±22	626±24

Figure 1. Measurement of hydroxyl radical generation from Fenton's reaction by X-band ESR spin trapping technique. (A) The computer-simulated spectrum for hydroxyl radical adduct (top). Hydroxyl radical was generated from H_2O_2 (0, 1, 10, 100, 250 μM) and $FeSO_4$ (0, 1, 10, 100, 250 μM) in DMEM-0 with the spin trap 5,5-dimethyl-1-pyrroline-*N*-oxide (DMPO; 50 mM). (B) The signal intensity (second peak of the spectrum) was normalized as the relative height against the signal intensity of the manganese oxide standard. Data are presented as mean ± SD of triplicate experiments. **Significantly different from the signal intensity generated from H_2O_2 and $FeSO_4$ (0 μM). $^{**}p < 0.01$ (Student's *t*-test). (C) Time-dependent hydroxyl radical generation from H_2O_2 (250 μM) and $FeSO_4$ (250 μM) in DMEM-0 with DMPO (220 mM). The ESR spectra of DMPO-OH spin adduct were obtained in 1, 2, 4, 5, 30 min after addition of H_2O_2. (D) The signal intensity (second peak of the spectrum) was normalized as the relative height against the signal intensity of the manganese oxide standard. The relative amount of hydroxyl radical was calculated by relative height against the signal intensity at 1 min after addition H_2O_2. Data are presented as mean ± SD of triplicate experiments. (E) HSC-2, HSC-3 and HSC-4 cells were seeded (5×10^3 cells/well) in 96-well plates. Nearly confluent cells were serum-starved overnight and the cells were cultured in DMEM-0 with various concentrations of H_2O_2 and/or $FeSO_4$ for 24 h. Cell viability was determined by the absorbance at 450 nm after 3 h incubation with Tetracolor ONE. Absorbance values were expressed as a percentage relative to untreated cells and the concentration of H_2O_2 and/or $FeSO_4$ resulting in 50% growth inhibition (IC_{50}) was calculated. All experiments were done in triplicate.

greater than those of H_2O_2 in the HNSCC cell lines (Figure 2A). We used HNSCC cells as a confirmatory experimental model because maximum changes in angiogenesis-related chemokine genes expressed by ROS treatment were demonstrated in HSC-2 cells. In addition, we also confirmed that the effects of H_2O_2 and/or $FeSO_4$ were dose-dependent (0–250 μM) in HSC-2 cells (Figure 2B).

To further clearly see the effects of ROS such as H_2O_2 and HO• on BRAK production, we determined the amount of BRAK with ELISA in HSC-2 cells. Both BRAK production levels in culture medium and cell layer were significantly decreased by treatment of H_2O_2 (250 μM). $FeSO_4$ itself also reduced BRAK levels in culture media and cell layers (Figure 3). Furthermore, the effect of HO• on the BRAK levels was much greater than that of H_2O_2 culture media and cell layers (Figure 3). These data indicated that BRAK mRNA levels correlated with BRAK production by treatment of H_2O_2 and HO• in HNSCC cells.

ROS effects on IL-8 and BRAK gene expression were attenuated by pre-treatment with N-acetyl-L-cysteine (NAC) in human HNSCC cells

N-acetyl-L-cysteine (NAC) is a thiol, a mucolytic agent, the precursor of L-cysteine and induces glutathione. NAC is known as an intracellular source of sulphydryl groups and is a common antioxidant *in vivo* where it scavenges ROS such as H_2O_2 and HO• [28].

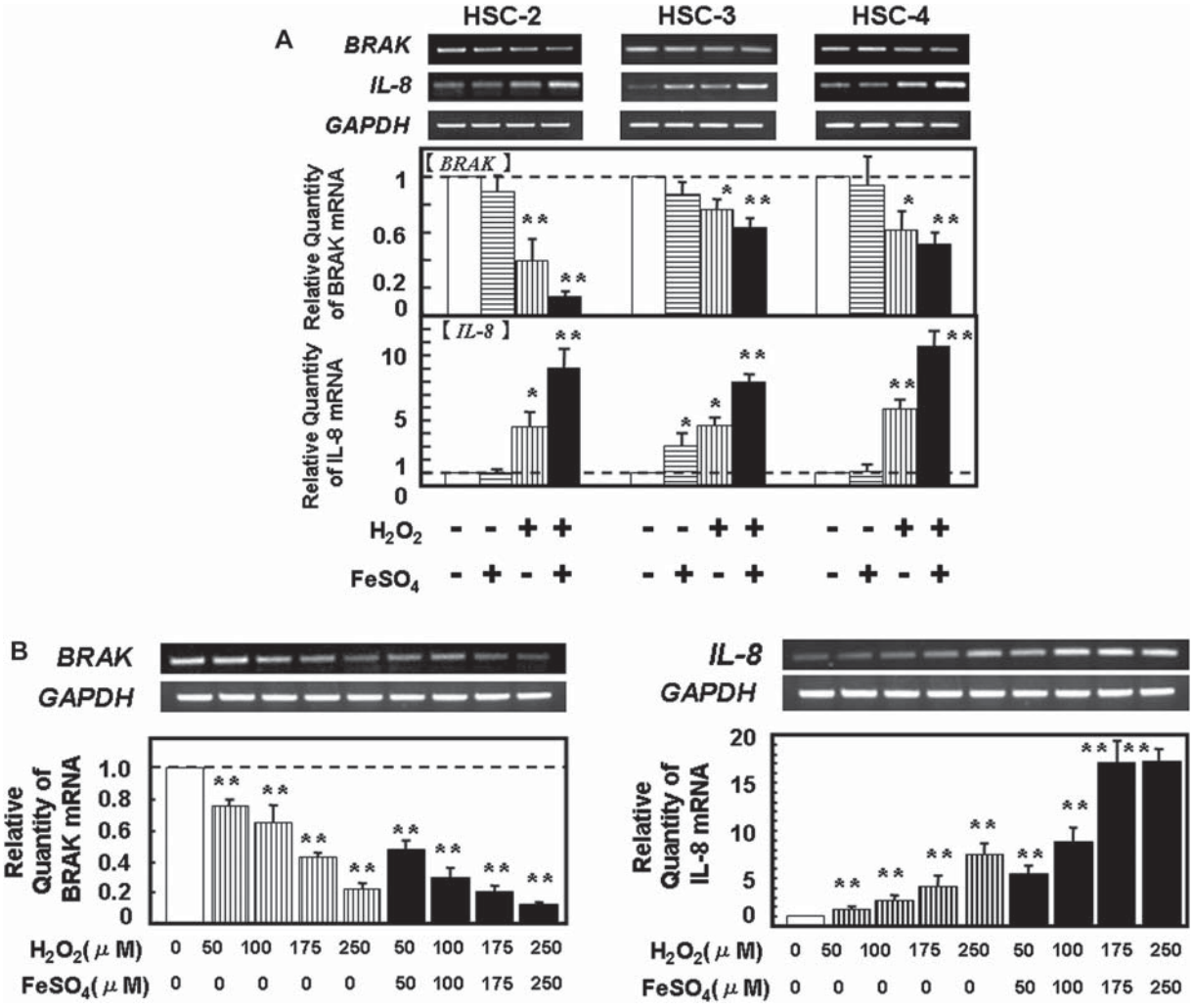

Figure 2. Reactive oxygen species regulate expression of angiogenesis related-chemokines in human HNSCC cells. (A) HSC-2, HSC-3 and HSC-4 cells were seeded (4×10^5 cells/well) in 35-mm diameter dishes. Nearly confluent cells were serum-starved overnight and the cells were cultured in DMEM-0 with H_2O_2 (250 μM) and/or $FeSO_4$ (250 μM) for 6 h. Total RNA was extracted after 6 h. After reverse transcription, BRAK, IL-8 and GAPDH mRNA levels were visualized by staining with ethidium bromide after separation by 2% agarose gel electrophoresis and real-time PCR analysis. The columns and bars represent mean ± SD in a triplicate assay. **Significantly different from control $^*p < 0.05$, $^{**}p < 0.01$, (Student's *t*-test). (B) Dose-dependent effects of H_2O_2 and/or $FeSO_4$ on BRAK and IL-8 mRNA levels. HSC-2 cells were seeded (4×10^5 cells/well) in 35-mm diameter dishes. Nearly confluent cells were serum-starved overnight, and the cells were cultured in DMEM-0 with various concentrations (50, 100, 175, 250 μM) of H_2O_2 (250 μM) and/or $FeSO_4$ (250 μM) for 6 h. Total RNA was extracted after 6 h. After reverse transcription, BRAK, IL-8 and GAPDH mRNA levels were visualized by staining with ethidium bromide after separation by 2% agarose gel electrophoresis and real-time PCR analysis. The columns and bars represent mean ± SD in a triplicate assay. **Significantly different from control $^{**}p < 0.01$, (Student's *t*-test).

To confirm whether changes in gene expression were induced by ROS, we used RT-PCR and real time PCR analysis to analyse the effects of ROS on BRAK and IL-8 gene expression in HNSCC cells pre-treated with NAC before ROS exposure. First, we measured the amount of total glutathione (GSH and GSSH), which is the most abundant intracellular ROS scavenger, following pre-treatment with NAC for 4 h. The amount of total glutathione was significantly increased by pre-treatment of HSC-2 cells with NAC (Figure 4A). Furthermore, ROS-induced changes in BRAK and IL-8 gene expression in HSC-2 cells were significantly attenuated by pre-treatment with NAC before H_2O_2 and $HO^\bullet$ exposure (Figure 4B).

ROS induces activation of EGF receptor–ERK pathway in HNSCC cells

To further elucidate the regulation of BRAK expression by ROS, we used Western blotting to examine the effects of ROS treatment of H_2O_2 and $HO^\bullet$ treatment on MAPK pathways (i.e. EGFR/MEK/ERK pathway) in HNSCC cells. EGF caused marked and rapid EGFR phosphorylation which reached maximal levels within as little as 30 min (Figure 5A), while EGFR phosphorylation induced by H_2O_2 and $HO^\bullet$ peaked at 1 h in HSC-2 cells (Figure 5B). We also confirmed phosphorylation of ERK1/2 downstream of EGFR. EGF-induced ERK1/2 phosphorylation

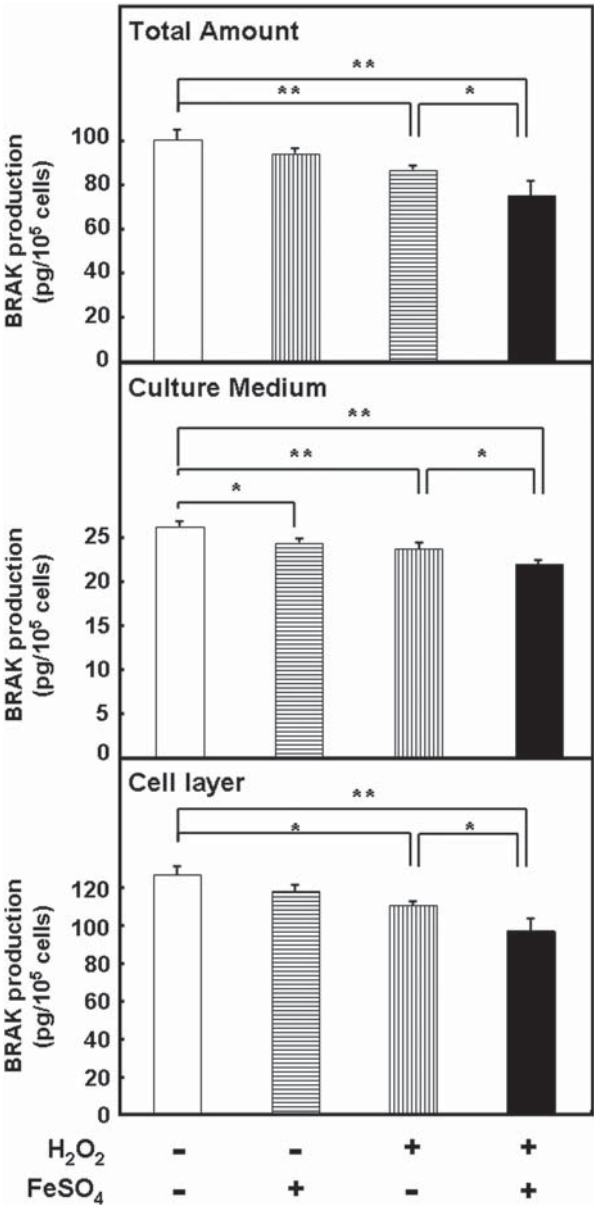

Figure 3. Reactive oxygen species decreased the production of BRAK in human HNSCC cells. HSC-2 cells were inoculated (4×10^5 cells/well) on a 35-mm diameter dish. Nearly confluent cells were serum-starved overnight and the cells were cultured in DMEM-0 with H_2O_2 (250 μM) and/or $FeSO_4$ (250 μM) for 48 h. These protein levels of BRAK were quantified using CXCL14 Duo Set ELISA Development System kits following the manufacturer's instruction. The columns and bars represent means ± SD in a triplicate assay. **Significantly different from the control, $^{*}p < 0.05$, $^{**}p < 0.01$, (Student's *t*-test).

peaked at 30 min (Figure 5A), whereas ERK1/2 phosphorylation induced by H_2O_2 and HO• peaked at 1–2 h in HSC-2 cells (Figure 5B).

Gefitinib attenuates ROS-induced gene expression of BRAK through activation of the EGFR-ERK phosphorylation pathway in HNSCC cells

The EGFR signalling pathway plays a crucial role in the aggressive features of human HNSCC cells [29]. *Therefore, EGFR was well known to a molecular therapeutic target for these types of cancer.* Gefitinib (ZD1839, Iressa), which is a tyrosine kinase inhibitor of EGFR, has been clinically used for the treatment of terminal patients with non-small cell lung cancer.

To determine whether ROS have influence on the EGFR-MEK-ERK signalling pathway, which correlates with the expression of BRAK mRNA, we used RT-PCR to examine the expression of BRAK and IL-8 in HNSCC cells in the presence of EGFR tyrosine kinase inhibitors, including ZD1839 and MEK tyrosine kinase inhibitors. The decrease in BRAK mRNA and increase in IL-8 mRNA caused by H_2O_2 and HO• treatment were inhibited in the presence of ZD1839 or PD153035 (Figures 6A and B). Furthermore, addition of the MEK tyrosine kinase inhibitors PD98059 or U0126 also reduced the effect of H_2O_2 and HO• on gene expression in HSC-2 cells (Figures 6C and D). The decrease in BRAK mRNA by ROS treatment was not affected by inhibitors of p38 or the NF-κB pathway. However, the induction of IL-8 mRNA by H_2O_2 and HO• in HNSCC cells was attenuated by inhibitors of p38 and NF-κB (data not shown). Collectively, our data indicates that the direct effects of oxidative stress on both BRAK and IL-8 are dependent on the EGFR-MEK-ERK signalling pathway.

Discussion

A clinical association between tumour angiogenesis and tumour development has been clearly demonstrated in a wide variety of tumour types including HNSCC [30]. It is well known that oxidative stress can occur through over-production of ROS and reactive nitrogen species through either endogenous or exogenous stimulants [31]. Oxidative stress induces a cellular redox imbalance which has been found to be present in various cancer cells to a greater extent than in normal cells; the redox imbalance may therefore be related to oncogenic stimulation [32]. However, little is known about how ROS such as H_2O_2 or HO• stimulate intracellular signalling, leading to the development of tumour cells caused by angiostatic/angiogenic chemokines. The results of the present study indicate that decreasing the expression of angiostatic chemokine CXCL14/BRAK would play a critical role in this signalling. ROS such as H_2O_2 or HO• directly reduced BRAK production in HSC-2 cells (Figure 3). ROS increase the cellular production of vascular endothelial growth factor and the angiogenic chemokine IL-8 in HNSCC cells [3]. We also confirmed that ROS directly up-regulated IL-8 mRNA levels (Figure 2). These results suggest that ROS may directly influence both angiostatic (i.e. BRAK) and angiogenic (i.e. IL-8) chemokines, resulting in malignant angiogenesis and tumour development. We found that the maximum changes

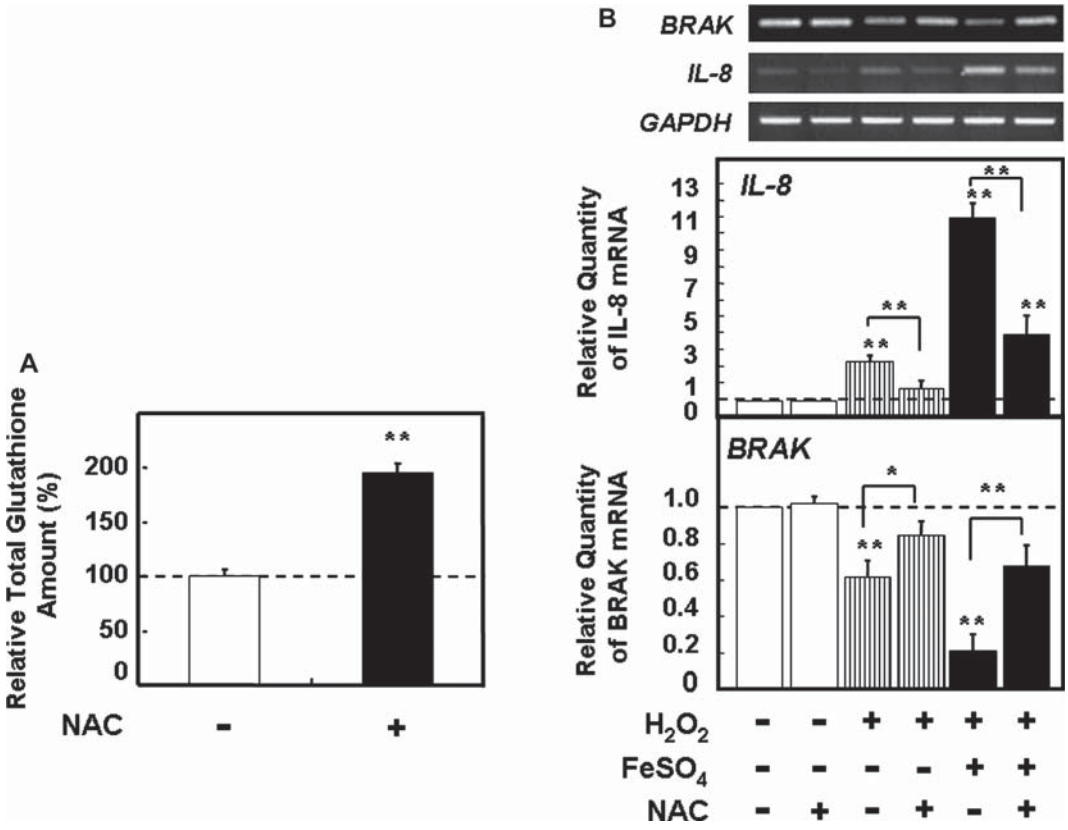

Figure 4. N-acetyl-L-cysteine (NAC) attenuates the effects of reactive oxygen species on expression of angiogenesis related-chemokines. (A) HSC-2 cells were seeded (4×10^5 cells/well) in 35-mm diameter dishes. Nearly confluent cells were serum-starved overnight. Total glutathione (GSH and GSSH) levels in HSC-2 cells were quantified using the Total Glutathione Quantification Kit. After treatment with or without NAC for 4 h, the cells were homogenized in 10 mM HCl and transferred to 96-well plates. Intracellular total glutathione levels were detected spectrophotometrically at 405 nm. (B) HSC-2 cells were pre-treated with NAC for 4 h and incubated with or without H_2O_2 (250 μM) and/or $FeSO_4$ (250 μM) for 6 h. Total RNA was extracted after 6 h. Following reverse transcription, BRAK, IL-8 and GAPDH mRNA levels were visualized by staining with ethidium bromide after separation by 2% agarose gel electrophoresis and real-time PCR analysis. The columns and bars represent mean ± SD in a triplicate assay. **Significantly different from the respective control, $^{*}p < 0.05$, $^{**}p < 0.01$.

in expression of angiogenesis-related chemokine genes, such as BRAK and IL-8, in response to ROS treatment were greater in HSC-2 cells than in HSC-3 and HSC-4 cells (Figure 2A). These phenomena were inhibited by the antioxidant NAC (Figure 4B), indicating the involvement of ROS in tumour angiogenesis in HNSCC cells.

The human chemokine BRAK was first isolated from breast and kidney cells by PCR cloning [6]. The precise function of BRAK is unknown because its receptor has not yet been identified [6,7]. The differentially-expressed BRAK gene was identical to the BRAK, which is ubiquitously expressed in normal tissue extracts but is absent from many tumour cell lines *in vitro* [6–8]. Expression of BRAK is decreased significantly in HNSCC cells treated with EGF [8]. To investigate the effect of ROS on BRAK expression, we examined the effects of H_2O_2 and $HO^{\bullet}$ on the EGFR/MEK/ERK pathway in HSC-2 cells. We confirmed that inhibition of EGFR tyrosine kinase by ZD1839 or PD153035 suppressed the induction of BRAK mRNA by ROS (Figure 6A). Further, PD98059 and U0126, which are MEK tyrosine kinase inhibitors, prevented the ROS-mediated induction of BRAK mRNA in HSC-2 cells (Figure 6C). These results indicate that ROS down-regulate BRAK mRNA via EGFR/MEK/ERK activation in HSC-2 cells (Figure 6).

EGFR was found to be a strong prognostic indicator in head and neck, ovarian, cervical, bladder, and oesophageal cancers. The 2,3,5-tris-(glutathione-S-yl) hydroquinone-mediated oxidative stress-induced phosphorylation of MAPKs, especially ERK1/2, required EGFR activation in renal proximal tubule epithelial cells [33]. Interestingly, the induction of EGFR phosphorylation by ROS peaked at 1 h in HSC-2 cells (Figure 5B). Furthermore, H_2O_2 and $HO^{\bullet}$ also induced ERK1/2 phosphorylation which peaked at 1–2 h in HSC-2 cells (Figure 5B). We confirmed that inhibition of EGFR tyrosine kinase by ZD1839 or PD153035 suppressed ROS-induced EGFR phosphorylation (Figure 6B). In addition, PD98059 or U0126 prevented ROS-mediated alterations in ERK1/2 phosphorylation in HSC-2 cells

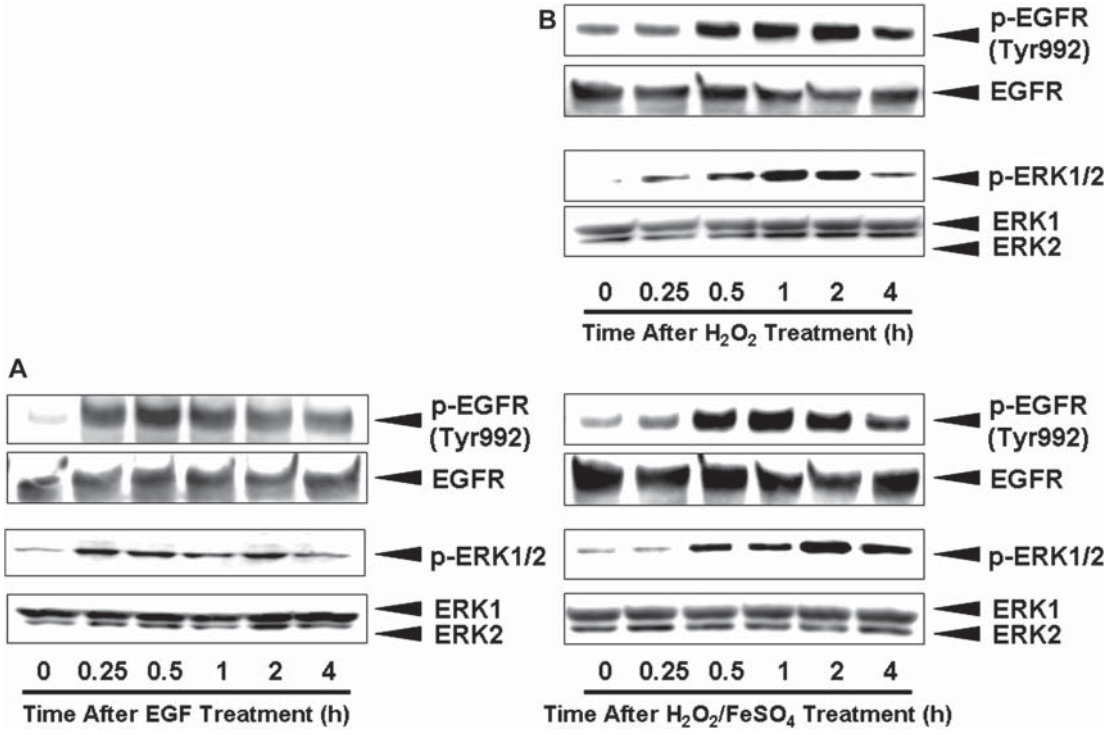

Figure 5. Time-dependent effects of EGF and reactive oxygen species on phosphorylation of EGFR and ERK1/2. HSC-2 cells were seeded (4×10^5 cells) in 35-mm diameter dishes. Nearly confluent cells were serum-starved overnight and the cells were treated with (A) EGF (10 ng/ml), (B) with or without H_2O_2 (250 μM) and/or $FeSO_4$ (250 μM) for 0.25, 0.5, 1, 2 or 4 h. Whole cell lysates were extracted and electrophoretically resolved on a polyacrylamide gradient (4–20%) gel and the activation of EGFR and ERK was analysed by Western blotting.

(Figure 6D). These observations suggest that ROS directly induce EGFR phosphorylation and ERK1/2 phosphorylation in HSC-2 cells (Figure 6).

Oxidative stress induced by ROS may also have important effects on p53, cell proliferation, invasiveness and metastasis [1]. Excessive amounts of ROS may arise either from excessive stimulation of NADPH oxidase or from less well-regulated sources such as the mitochondrial electron-transport chain [34]. The increased ROS in cancer cells may in turn affect certain redox sensitive molecules and further lead to significant consequences such as stimulation of cellular proliferation, cell differentiation, alteration in sensitivity to angiogenesis during promotion of mutation and genetic instability and carcinogenesis [1,31,34]. Indeed, knockout mice that genetically lack various antioxidant enzymes show enhanced oxidative damage and age-related cancer development. Direct oxidative damage to DNA by certain ROS, such as H_2O_2 and $HO^{\bullet}$, has been implicated in oncogenesis [1]. However, most studies on the effects of oxidative stress have examined the effects of H_2O_2, rather than $HO^{\bullet}$, on cellular proliferation, differentiation and angiogenesis in carcinoma cell lines. The present study showed that BRAK and IL-8 gene expression was altered dose-dependently (0–250 μM) by H_2O_2 and/or $FeSO_4$ in HSC-2 cells (Figure 2B). The effects of $HO^{\bullet}$ treatment on the expression of the two angiogenesis related-chemokine genes were much greater than those of H_2O_2 in the three HNSCC cell lines, especially in HSC-2 cells (Figure 2). These results are consistent with the possibility that $HO^{\bullet}$ causes greater expression of angiogenesis related-chemokine and leads to oxidative damage to DNA and other malignant signalling in cancer cells.

Under normal physiological conditions, $O_2^{\bullet-}$ rapidly dismutates via enzymatic catalysis by SOD (equation 1). $HO^{\bullet}$ can be formed by the Haber-Weiss reaction from $O_2^{\bullet-}$ and H_2O_2 (equation 2); however, this reaction is considered to be too slow to compete with the dismutation reaction (equations 1 [35]).

$$O_2^{\bullet-} + O_2^{\bullet-} + 2H^+ \rightarrow H_2O_2 + O_2 \quad (1)$$

$$O_2^{\bullet-} + H_2O_2 \rightarrow O_2 + HO^{\bullet} + OH^- \quad (2)$$

$HO^{\bullet}$ can be generated more efficiently via the Haber-Weiss reaction if iron ions are present, a reaction known as the biological Fenton reaction (equations 3 and 4).

$$O_2^{\bullet-} + Fe^{3+} \rightarrow O_2 + Fe^{2+} \quad (3)$$

$$Fe^{2+} + H_2O_2 \rightarrow Fe^{3+} + HO^{\bullet} + OH^- \quad (4)$$

Inflammatory cells such as TAMs and neutrophils caused excessive ROS production resulting in

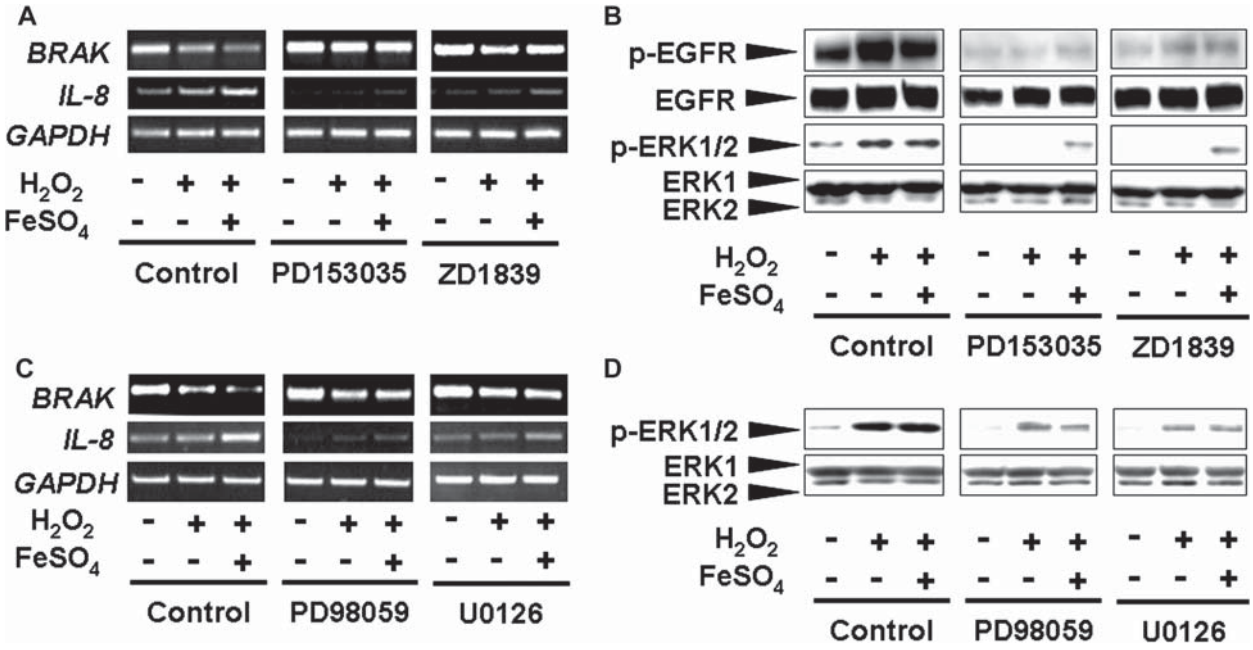

Figure 6. Reactive oxygen species regulate expression of angiogenesis related-chemokines through phosphorylation of EGFR and ERK1/2. HSC-2 cells were seeded (4×10^5 cells) in 35-mm diameter dishes. Nearly confluent cells were serum-starved overnight and the cells were cultured with or without H_2O_2 (250 μM) and/or $FeSO_4$ (250 μM) for 30 min (B, D) or 6 h (A, C) with or without pre-treatment with EGFR inhibitors [PD153035 (10 μM) or ZD1839 (1 μM)] (A, B) or MEK inhibitors [PD98059 (50 μM) or U0126 (10 μM)] (C, D) for 1 h. (A, C) Total RNA was extracted after 6 h. Following reverse transcription, BRAK, IL-8 and GAPDH mRNA levels were visualized by staining with ethidium bromide after separation by 2% agarose gel electrophoresis. (B, D) Whole cell lysates were extracted at 30 min electrophoretically resolved on a polyacrylamide gradient (4–20%) gel and analysed for activation of EGFR and ERK with Western blotting.

damage to DNA and other biomolecules, which can promote malignancy of the tumour cell, including HNSCC cells [1,10–14]. It has been suggested that H_2O_2 can activate tumour cell signalling, especially via NF-κB [15], studies exploring the role of ROS in tumour cell signalling to date have used H_2O_2. Furthermore, $HO^{\bullet}$ can be generated by TAMs via the Fenton/Haber-Weiss reaction in the presence of Fe^{2+} and Cu^{2+} in tumour tissue [1–4,16]. $HO^{\bullet}$ is one of the strong oxidizing agents among ROS and ROS levels are known to correlate with tumour development [1,14,17,18]. The unregulated or prolonged production of cellular oxidants has been linked to mutation (induced by oxidant-induced DNA damage), as well as modification of gene expression. Collectively, our data indicate that oxidative stress induced by H_2O_2 and $HO^{\bullet}$ not only leads to angiogenesis via the expression of angiogenic chemokines such as IL-8, but also impaired anti-angiogenesis mechanisms through reduced expression of the angiostatic chemokine BRAK in HNSCC cells (Figure 6). In addition, the effects of $HO^{\bullet}$ on the expression of angiogenesis-related chemokines were greater than those of H_2O_2.

We plan to focus on the emerging role of the so-called 'labile' (redox active) form of iron in ROS-mediated signalling in relation to cancer development [36]. It is possible that ferrous or ferric iron in the Fenton system may have been responsible for the effects on gene expression observed in the present study. Indeed, we confirmed that $FeSO_4$ itself down-regulated BRAK gene expression (Figure 3). Regarding total BRAK protein in culture media and cell layers, we observed that the levels were reduced to a greater extent by $HO^{\bullet}$ generated from the Fenton reaction than by $FeSO_4$ or H_2O_2 alone (Figure 3), indicating that $HO^{\bullet}$ had a greater effect than H_2O_2 on expression of BRAK and IL-8 genes in HNSCC cells (Figure 3). Overall, these data show that $HO^{\bullet}$ is a potent modulator of angiogenesis-related chemokines in HNSCC cells. In addition, we also confirmed that $O_2^{\bullet-}$ affects the expression of BRAK in HNSCC cells. BRAK mRNA levels were significantly decreased by $O_2^{\bullet-}$ treatment (unpublished data). Further studies are needed to determine the mechanisms by which $O_2^{\bullet-}$ reduces BRAK mRNA levels.

In conclusion, our findings indicated that oxidative stress induced by ROS such as H_2O_2 and $HO^{\bullet}$ directly stimulates not only a decrease in the expression of BRAK but also an increase of IL-8 expression in HNSCC cells. These results suggest that oxidative stress induces angiogenesis and tumour progression by regulating the expression of both angiostatic (BRAK) and angiogenic (IL-8) chemokine genes in HNSCC cells. These observations indicate that sustained or constitutive ROS production is prevalent in cancer cell lines and that this contributes to

malignant progression and therapeutic resistance in the most major human cancer cell types, especially HNSCC cells.

Declaration of interest: Supported by grants from High-Tech Research Center Project of Kanagawa Dental College, Yokosuka, Kanagawa, Japan and Grants-in-Aid for Scientific Research from the Japanese Ministry of Education, Science, and Culture to 16791169, 18890213, 21390543 and 19592371.

References

[1] Halliwell B. Oxidative stress and cancer: have we moved forward. Biochem J 2007;401:1–11.

[2] Bradburn JE, Pei P, Kresty LA, Lang JC, Yates AJ, McCormick AP, Mallery SR. The effects of reactive species on the tumorigenic phenotype of human head and neck squamous cell carcinoma (HNSCC) cells. Anticancer Res 2007;27:3819–3827.

[3] Brat DJ, Bellail AC, Van Meir EG. The role of interleukin-8 and its receptors in gliomagenesis and tumoral angiogenesis. Neuro Oncol 2005;7:122–133.

[4] Shurin GV, Ferris RL, Tourkova IL, Perez L, Lokshin A, Balkir L, Collins B, Chatta GS, Shurin MR. Loss of new chemokine CXCL14 in tumor tissue is associated with low infiltration by dendritic cells (DC), while restoration of human CXCL14 expression in tumor cells causes attraction of DC both *in vitro* and *in vivo*. J Immunol 2005;174: 5490–5498.

[5] Sleeman MA, Fraser JK, Murison JG, Kelly SL, Prestidge RL, Palmer DJ, Watson JD, Kumble KD. B cell- and monocyte-activating chemokine (BMAC), a novel non-ELR alpha-chemokine. Int Immunol 2000;12:677–689.

[6] Hromas R, Broxmeyer HE, Kim C, Nakshatri H, Christopherson K, 2nd, Azam M, Hou YH. Cloning of BRAK, a novel divergent CXC chemokine preferentially expressed in normal versus malignant cells. Biochem Biophys Res Commun 1999;255:903–906.

[7] Frederick MJ, Henderson Y, Xu X, Deavers MT, Sahin AA, Wu H, Lewis DE, El-Naggar AK, Clayman GL. *In vivo* expression of the novel CXC chemokine BRAK in normal and cancerous human tissue. Am J Pathol 2000;156: 1937–1950.

[8] Ozawa S, Kato Y, Komori R, Maehata Y, Kubota E, Hata R. BRAK/CXCL14 expression suppresses tumor growth *in vivo* in human oral carcinoma cells. Biochem Biophys Res Commun 2006;348:406–412.

[9] Knaapen AM, Gungor N, Schins RP, Borm PJ, Van Schooten FJ. Neutrophils and respiratory tract DNA damage and mutagenesis: a review. Mutagenesis 2006;21:225–236.

[10] Liss C, Fekete MJ, Hasina R, Lam CD, Lingen MW. Paracrine angiogenic loop between head-and-neck squamous-cell carcinomas and macrophages. Int J Cancer 2001;93:781–785.

[11] Sica A, Bronte V. Altered macrophage differentiation and immune dysfunction in tumor development. J Clin Invest 2007;117:1155–1166.

[12] Lee C, Miura K, Liu X, Zweier JL. Biphasic regulation of leukocyte superoxide generation by nitric oxide and peroxynitrite. J Biol Chem 2000;275:38965–38972.

[13] Lee CI, Liu X, Zweier JL. Regulation of xanthine oxidase by nitric oxide and peroxynitrite. J Biol Chem 2000;275: 9369–9376.

[14] Brown NS, Bicknell R. Hypoxia and oxidative stress in breast cancer. Oxidative stress: its effects on the growth, metastatic potential and response to therapy of breast cancer. Breast Cancer Res 2001;3:323–327.

[15] Gloire G, Legrand-Poels S, Piette J. NF-kappaB activation by reactive oxygen species: fifteen years later. Biochem Pharmacol 2006;72:1493–1505.

[16] Huang X. Iron overload and its association with cancer risk in humans: evidence for iron as a carcinogenic metal. Mutat Res 2003;533:153–171.

[17] Hagiwara T, Lee CI, Okabe E. Differential sensitivity to hydroxyl radicals of pre- and postjunctional neurovascular transmission in the isolated canine mesenteric vein. Neuropharmacol 2000;39:1662–1672.

[18] Lee C, Okabe E. Hydroxyl radical-mediated reduction of Ca(2+)-ATPase activity of masseter muscle sarcoplasmic reticulum. Jpn J Pharmacol 1995;67:21–28.

[19] Nicholson RI, Gee JM, Harper ME. EGFR and cancer prognosis. Eur J Cancer 2001;37(Suppl 4):S9–S15.

[20] Aslan M, Ozben T. Oxidants in receptor tyrosine kinase signal transduction pathways. Antioxidants Redox Signal 2003;5: 781–788.

[21] Lee MC, Shoji H, Komatsu T, Yoshino F, Ohmori Y, Zweier JL. Inhibition of superoxide generation from fMLP-stimulated leukocytes by high concentrations of nitric oxide or peroxynitrite: characterization by electron spin resonance spectroscopy. Redox Rep 2002;7:271–275.

[22] Lee MC, Shoji H, Miyazaki H, Yoshino F, Hori N, Miyake S, Ikeda Y, Anzai K, Ozawa T. Measurement of oxidative stress in the rodent brain using computerized electron spin resonance tomography. Magn Reson Med Sci 2003;2:79–84.

[23] Lee MC, Shoji H, Miyazaki H, Yoshino F, Hori N, Toyoda M, Ikeda Y, Anzai K, Ikota N, Ozawa T. Assessment of oxidative stress in the spontaneously hypertensive rat brain using electron spin resonance (ESR) imaging and *in vivo* L-Band ESR. Hypertens Res 2004;27:485–492.

[24] Miyazaki H, Shoji H, Lee MC. Measurement of oxidative stress in stroke-prone spontaneously hypertensive rat brain using *in vivo* electron spin resonance spectroscopy. Redox Rep 2002;7:260–265.

[25] Kobayashi K, Yoshino F, Takahashi SS, Todoki K, Maehata Y, Komatsu T, Yoshida K, Lee MC. Direct assessments of the antioxidant effects of propofol medium chain triglyceride/long chain triglyceride on the brain of stroke-prone spontaneously hypertensive rats using electron spin resonance spectroscopy. Anesthesiology 2008;109:426–435.

[26] Rikimaru K, Toda H, Tachikawa N, Kamata N, Enomoto S. Growth of the malignant and nonmalignant human squamous cells in a protein-free defined medium. *In Vitro* Cell Dev Biol 1990;26:849–856.

[27] Maehata Y, Takamizawa S, Ozawa S, Izukuri K, Kato Y, Sato S, Lee MC, Kimura A, Hata R. Type III collagen is essential for growth acceleration of human osteoblastic cells by ascorbic acid 2-phosphate, a long-acting vitamin C derivative. Matrix Biol 2007;26:371–381.

[28] Zafarullah M, Li WQ, Sylvester J, Ahmad M. Molecular mechanisms of N-acetylcysteine actions. Cell Mol Life Sci 2003;60:6–20.

[29] Koppikar P, Choi SH, Egloff AM, Cai Q, Suzuki S, Freilino M, Nozawa H, Thomas SM, Gooding WE, Siegfried JM, Grandis JR. Combined inhibition of c-Src and epidermal growth factor receptor abrogates growth and invasion of head and neck squamous cell carcinoma. Clin Cancer Res 2008; 14:4284–4291.

[30] Baba Y, Kato Y, Mochimatsu I, Nagashima Y, Kurihara M, Kawano T, Taguchi T, Hata R, Tsukuda M. Inostamycin suppresses vascular endothelial growth factor-stimulated growth and migration of human umbilical vein endothelial cells. Clin Exp Metastasis 2004;21:419–425.

[31] Klaunig JE, Kamendulis LM. The role of oxidative stress in carcinogenesis. Annu Rev Pharmacol Toxicol 2004;44:239–267.

[32] Valko M, Rhodes CJ, Moncol J, Izakovic M, Mazur M. Free radicals, metals and antioxidants in oxidative stress-induced cancer. Chem-Biol Interact 2006;160:1–40.
[33] Ramachandiran S, Huang Q, Dong J, Lau SS, Monks TJ. Mitogen-activated protein kinases contribute to reactive oxygen species-induced cell death in renal proximal tubule epithelial cells. Chem Res Tox 2002;15:1635–1642.
[34] Droge W. Free radicals in the physiological control of cell function. Physiol Rev 2002;82:47–95.
[35] Thomas MJ, Mehl KS, Pryor WA. The role of the superoxide anion in the xanthine oxidase-induced autoxidation of linoleic acid. Biochem Biophys Res Commun 1978;83:927–932.
[36] Galaris D, Skiada V, Barbouti A. Redox signaling and cancer: the role of 'labile' iron. Cancer Lett 2008;266:21–29.